Journal of the Taiwan Institute of Chemical Engineers 83 (2018) 124–132

Contents lists available at ScienceDirect

Journal of the Taiwan Institute of Chemical Engineers

journal homepage: www.elsevier.com/locate/jtice

Phosphorous recovery by means of fluidized bed homogeneous crystallization of calcium phosphate. Influence of operational variables and electrolytes on brushite homogeneous crystallization

Patrick S. Caddarao [a], Sergi Garcia-Segura [b], Florencio C. Ballesteros Jr [a], Yao-Hui Huang [c], Ming-Chun Lu [b,*]

[a] Environmental Engineering Graduate Program, College of Engineering, University of the Philippines, Diliman, Quezon City, Philippines
[b] Department of Environmental Resources Management, Chia-Nan University of Pharmacy and Science, Tainan 71710, Taiwan
[c] Department of Chemical Engineering, Sustainable Environment Research Center, National Cheng Kung University, Tainan, Taiwan

ARTICLE INFO

Article history:
Received 26 September 2017
Revised 7 December 2017
Accepted 8 December 2017
Available online 26 December 2017

Keywords:
Fluidized-bed reactor
Phosphate homogeneous crystallization
Water treatment technologies
Granulation process
Phosphate removal

ABSTRACT

Phosphate recovery from wastewaters is one of the major engineering challenges to securing the worldwide food production. Fluidized-bed heterogeneous crystallization of struvite has been one of the most considered technologies. Nevertheless, the recovery of other phosphate products could be of the major interest at industrial level. Thus, in this work we present the recovery of calcium phosphate salts as brushite by a novel fluidized-bed homogeneous crystallization (FBHC) process. The no requirement of seeds in FBHC reactor allows obtaining high-purity crystals. The operational parameters of the FBHC process have been optimized in order to achieve the higher degree of granulation and to obtain the most homogeneous distribution of granules sizes. Thus, the treatment of 1500 mg/L of phosphate at pH 9.0 with a ratio of 1.2:1.0 of $[Ca^{2+}]$:$[PO_4{}^{3-}]_T$ leads to the obtaining of ca. 90% of granulation with crystals of 0.5 mm of diameter. The influence of electrolytes typically found in TFT-LCD industry has been further considered. The characterization of the spheroidal crystals obtained allowed identifying brushite (calcium hydrogenphosphate salt) as unique crystal phase.

1. Introduction

Phosphorous is an indispensable chemical in fertilizers composition along with nitrogen species. Unlike nitrogen, phosphorous is a non-renewable resource [1–3]. The mining extraction of phosphate rocks is depleting dramatically mineral reserves. Thus, ascertaining phosphorous sources will not become only an engineering challenge but also of high social relevance in order to securing worldwide food production [1].

Phosphorous in wastewaters contributes to the eutrophication of waters [4,5]. About 90% of incoming phosphorous in water treatment plants is lost in the form of sewage sludge [6–8]. The development of water treatment technologies able to recover phosphate for its reuse in industrial manufacturing processes could contribute in a double beneficial way: (i) removal of phosphorous as pollutant from water sources, and (ii) secondary alternative phosphorous source. Phosphorous removal has been considered by using different technologies such filtration [9,10], coagulation [11], electrocoagulation [12,13], electrodyalisis [14], capacitive deionization [15] or biological treatments with photosynthetic organisms [16,17]. The mentioned processes do not allow phosphorous recovery for reuse.

Precipitation is a low-cost and highly efficient methodology for phosphorous removal. Unfortunately, the recovery of phosphorous from the precipitation sludge with high moisture content is not possible. Fluidized-bed crystallization (FBC) emerges as a promising environmental-friendly technology of phosphorous recovery [2,6,20,22]. FBC presents several advantages in front of conventional precipitation such as the use of fewer chemicals and the obtaining of crystallized particles (granules). Fluidized-bed reactors have been applied to the treatment of wastewaters containing inorganic pollutants such as Ni^{2+}[27,28], Cu^{2+}[29], Pb^{2+} [30,31], fluoride [32,33] and phosphorous [34,35]. The main disadvantage of FBC is that crystals grow onto supports (seeds). The different composition of these seeds leads to unpurified products that would inevitably affect the recyclability of the recovered crystals by FBC [30,32,34]. This work presents phosphorous recovery by a novel process without seeds so-called fluidized-bed homogeneous crystallization (FBHC). Here, the final product is obtained solely

* Corresponding author.
E-mail addresses: mmclu@mail.cnu.edu.tw, mclu@ms17.hinet.net (M.-C. Lu).

https://doi.org/10.1016/j.jtice.2017.12.009
1876-1070/

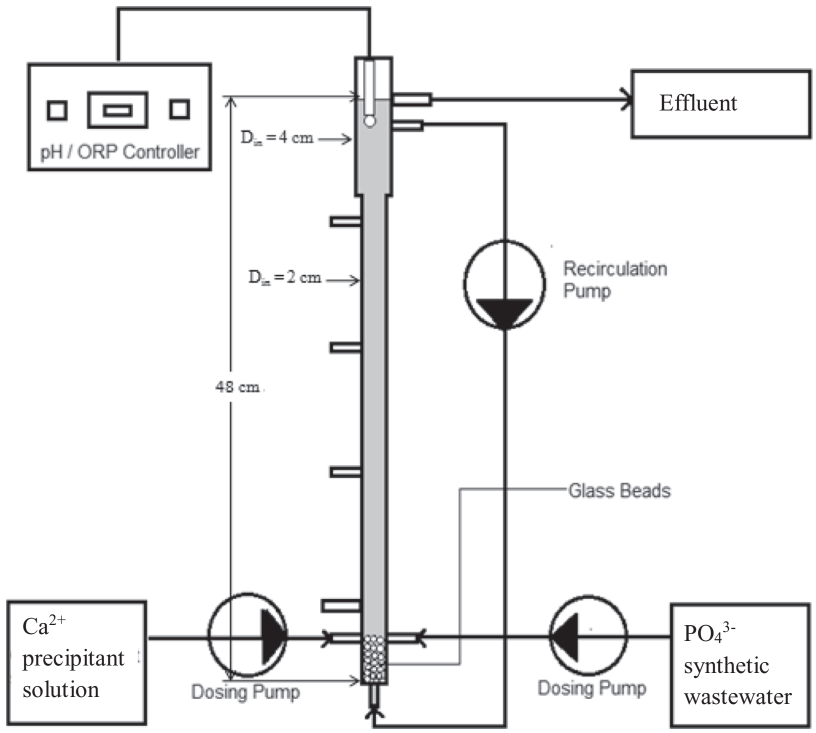

Fig. 1. Scheme of fluidized-bed reactor for homogeneous crystallization.

by homogeneous crystallization instead of conventional heterogeneous growing of the product onto the active surface of seed material [7,28,30]. FBHC is conducted under mild conditions of supersaturation where moderate amounts of fine nuclei agglomerate forming sufficient active sites to promote homogeneous crystal growth of high-purity granules. The main differences of FBHC to conventional technologies should be highlighted as (i) sludge is not produced, (ii) phosphorous is not only removed but recovered, and (iii) high pure granules are produced.

The formation of insoluble phosphate salts such struvite magnesium ammonium phosphate ($K_{ps} = 7.58 \times 10^{-14}$) is known because its natural precipitation in the sludge pipes at water-treatment plants [2,4,6,18–20]. However, other phosphate salts should be considered because of their interest from industrial/manufacturing points of view [8, 21–23]. Calcium phosphates (brushite) is used for several medical/biological applications as bioceramic in orthopedic and dental application, cancer therapies, food additive and biotechnological applications [24,25]. Furthermore, brushite is a phosphorous source for fertilizer or phosphoric acid manufacture [26].

In this work, obtaining of brushite crystals from synthetic effluents was studied by means of FBHC process. Variables of influence were studied in order to optimize removal with major granulation percentages. FBHC was conducted in presence of different electrolytes typically found in TFT-LCD industry effluents to evaluate the feasible application of this technology on the treatment of actual effluents. The characterization of the crystals allowed a better understanding of brushite crystallization mechanism and FBHC process.

2. Experimental

2.1. Chemicals

Phosphate solutions were prepared with KH_2PO_4 of high purity degree (>99.5%) purchased from Merck. Calcium chloride (96% purity) used as precipitant was supplied by Ferak Berlin GmbH. Reaction zone pH was maintained by the addition of little amounts of NaOH or HCl acquired from Merck. Ammonium molybdate tetrahydrated, potassium antimony (III) oxide tartrate trihydrate, and L(+)-Ascorbic acid of analytical grade used in the colorimetric quantification of phosphate were purchased from Panreac. The electrolytes used to simulate the industrial effluent were of analytical grade supplied by Sigma-Aldrich. All solutions were prepared using high-purity water from a Millipore Milli-Q system with resistivity > 18 MΩ cm.

2.2. Fluidized-bed homogeneous crystallization reactor

The fluidized-bed reactor (Fig. 1) consisted of a 550 mL cylindrical glass tube reactor divided in two sections: (i) Lower section of 80 cm height and 2 cm of inner diameter, (ii) upper section of 15 cm height and 4 cm of inner diameter. The treated solution was recirculated through the reactor with a peristaltic pump at variable flow rate to ensure fluidization of obtained granules. Achieving fluidization conditions is mandatory to ensure the formation of insoluble granules. Thus, up-flow solution recirculated should surpass the minimum fluid velocity (U_{mf}) where the flow compensate the gravitational force of the particles maintaining the particles in fluidized state [30,36,37]. For a low Reynolds (*Re*) number, as applied in FBHC process, the U_{mf} can be defined by expression (1).

$$U_{mf} = [0.0007(Re)_{mf}{}^{-0.063}]\frac{g d_p{}^2(\rho_p - \rho_f)}{\mu} \quad (1)$$

where g is the gravitational acceleration, d_p is the equivalent particle diameter, ρ_p is the particles density, ρ_f is the fluid density and μ is the fluid viscosity. Due to the nucleation, nuclei agglomeration and crystal growth mechanism, the particles change their d_p in function of time. Consequently, recirculation flow should be modified according to $(\delta d_p/\delta_t)$ variation to maintain the granules in the fluidization state. Fluidization state was ascertained by

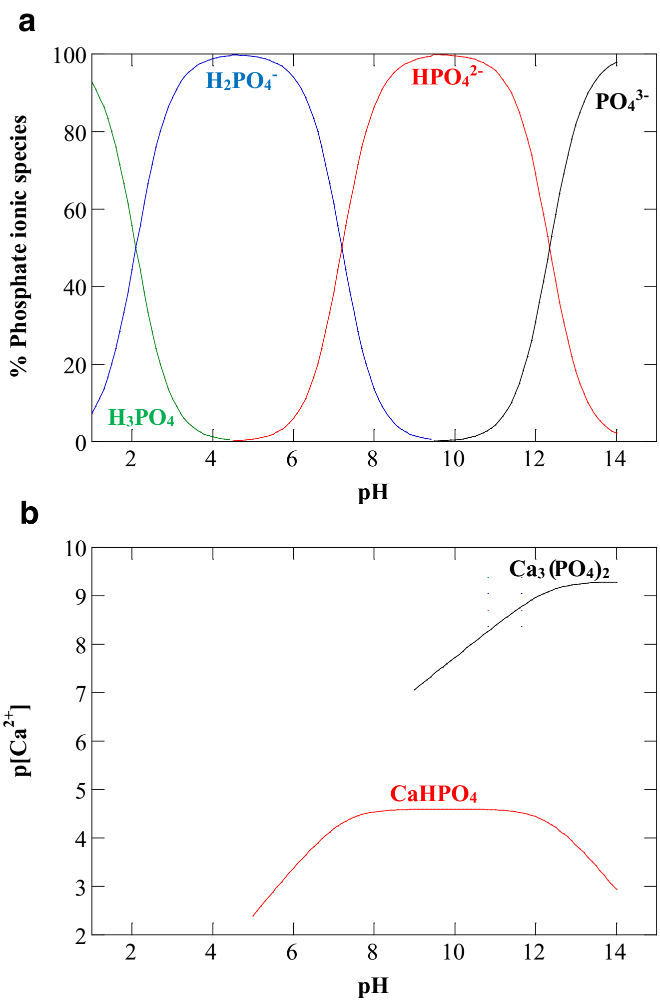

Fig. 2. (a) Phosphate anionic species distribution in function of pH. (b) Minimum concentration of precipitant ([Ca^{2+}]) required to initiate precipitation of insoluble phosphate salts.

maintaining formed granules under 50% bed expansion within the fluidized-bed reactor.

Glass beads were added at the bottom of the reactor as turbulence promoters to prevent sever clogging; avoid bubbles formation in distributor holes and to improve flow distribution. The precipitant was always added in excess to ensure $[PO_4^{3-}]_T$ conversion into calcium phosphate. Samples were filtered with 0.45 µm membranes and mixed with 30 µL of concentrated HNO_3 prior dissolved phosphate and calcium ions quantification. Total phosphate and calcium (including fines) were determined from unfiltered samples. Phosphate removal and phosphate granulation were estimated according to Eqs. (2) and (3) [7,30]:

$$\%\text{Removal} = \frac{[P]_0 - [P_D]_t}{[P]0} \times 100 \quad (2)$$

$$\%\text{Granulation} = \frac{[P]_0 - [P_D]_t}{[P]0} \times 100 \quad (3)$$

where $[P]_0$ is the initial phosphate content, $[P_D]_t$ is the dissolved phosphate in solution at treatment time *t* and $[P_T]_t$ the total phosphate in solution including fines and solids in suspension (not granules) at treatment time *t*, respectively.

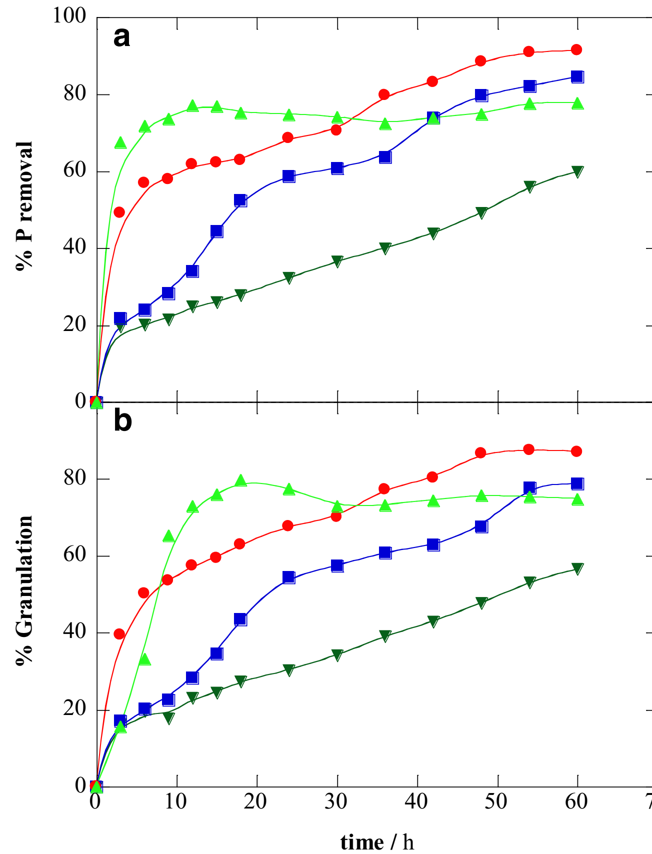

Fig. 3. Percentage of (a) phosphorus removal and (b) granulation achieved by means of FBHC vs time of operation on the treatment of 1500 mg/L solutions of phosphate with a molar ratio of 1.2:1.0 [Ca^{2+}]:$[PO_4^{3-}]_T$ −under different pH: (▼) 6.0, (■) 7.0, (●) 9.0 and (▲)11.0.

2.3. Instruments and analytical procedures

Solution pH was continuously monitored by a pH/ORP controller PC-310 from Shin Shiang Tech Instruments. Phosphate in solution was quantified by spectrophotometric analysis according to the phosphomolybdenum blue method at 698 nm [38] with a Genesys 20 UV–Vis spectrophotometer of Thermo Spectronic. Calcium cation concentration was quantified by atomic absorption spectrometry with a Lumina® hollow cathode lamp using an AAnlayst 200 Atomic Absorption Spectrometer of Perkin Elmer. Obtained granules were recovered, dried at 37 °C, and sieved to define particle size distribution using Mechanical Sieve Series. Granules were characterized by Scanning Electron Microscopy (SEM) using a Quanta 200 SEM from FEI Company. Crystalline phase characterization was conducted by X-Ray Diffraction (XRD) analysis with a Rigaku DX-2000 SSC diffractometer by applying a Cu $K\alpha_{1+2}$ radiation ($\lambda(\alpha_1) = 0.154060$ nm and $\lambda(\alpha_2) = 0.154443$ nm) at 40 kV and 30 mA current.

3. Results and discussion

3.1. Influence of pH on phosphate recovery

Two insoluble calcium phosphate salts could be obtained: (i) Calcium hydrogenphosphate formed from reaction (4); and (ii) calcium phosphate precipitated following reaction (5). Their respective solubility product constants (K_{sp}) could be expressed by means of Eq. (6) and (7), respectively [25]:

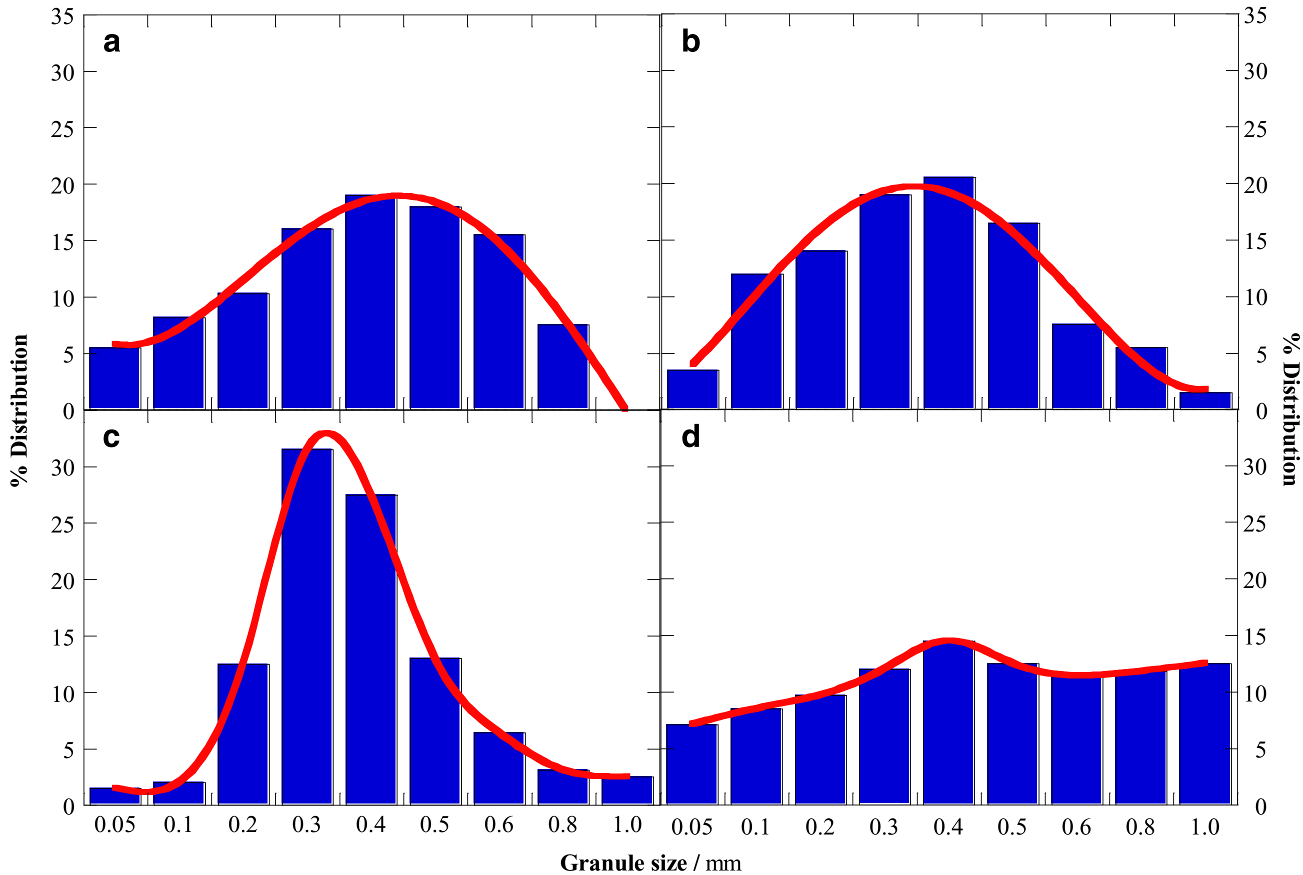

Fig. 4. Size distribution of granules obtained from experiences of Fig. 3 at different pH: (a) 6.0, (b) 7.0, (c) 9.0 and (d) 11.0.

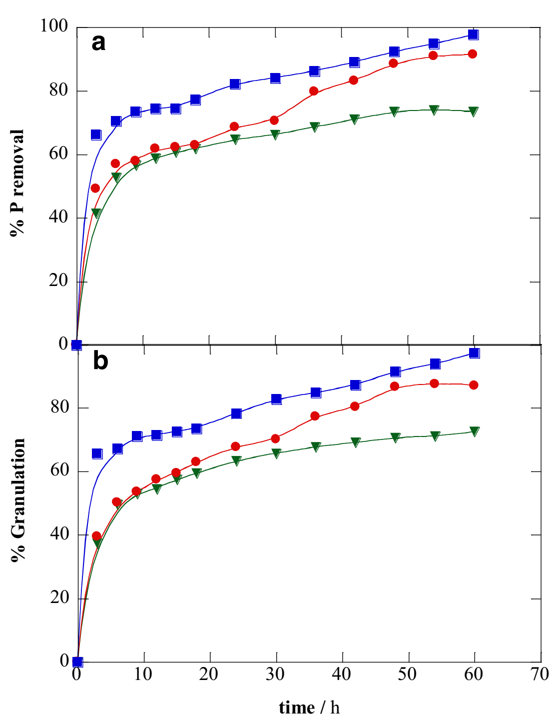

Fig. 5. Percentage of (a) phosphorus removal and (b) granulation achieved by means of FBHC vs time on the treatment of 1500 mg/L solutions of phosphate at pH 9.0 with different molar ratio of $[Ca^{2+}]:[PO_4^{3-}]_T$: (▼) 1.0:1.0, (●) 1.2:1.0 and (■) 1.4:1.0.

$$Ca^{2+} + HPO_4^{2-} \leftrightharpoons CaHPO_4 \tag{4}$$

$$3\ Ca^{2+} + 2\ PO_4^{3-} \leftrightharpoons Ca_3\ (PO_4)_2 \tag{5}$$

$$K_{sp} = \frac{a_{Ca^{2+}}\, a_{HPO_4^{2-}}}{a_{CaHPO_4}} = \left[Ca^{2+}\right]\left[HPO_4^{2-}\right] = 1.0 \times 10^{-7} \tag{6}$$

$$K_{sp} = \frac{(a_{Ca^{2+}})^3 \left(a_{PO_4^{3-}}\right)^2}{a_{Ca_3(PO_4)_2}} = \left[Ca^{2+}\right]^3\left[PO_4^{3-}\right]^2 = 2.07 \times 10^{-33} \tag{7}$$

where a_i are the activity of the different species involved in the precipitation reaction. Solid species activity could be considered equal to the unity and simplified. Under diluted concentration of ionic species, such in the FBHC operational conditions, their activities could be considered approximately equal to their concentrations [30].

The pH affects species distribution in solution, being of indisputable relevance on the crystallization processes of phosphate species. Phosphoric acid presents three different pK_a values for the dissociation of the protons of $pK_{a1} = 2.15$, $pK_{a2} = 7.20$ and $pK_{a3} = 12.35$ for reactions (8)–(10), respectively.

$$H_3PO_4 \leftrightharpoons H^+ + H_2PO_4^- \tag{8}$$

$$H_2PO_4^- \leftrightharpoons H^+ + HPO_4^{2-} \tag{9}$$

$$HPO_4^{2-} \leftrightharpoons H^+ + PO_4^{3-} \tag{10}$$

Fig. 2a shows the speciation distribution of phosphate anionic species determined in function of pH. It can be inferred that to

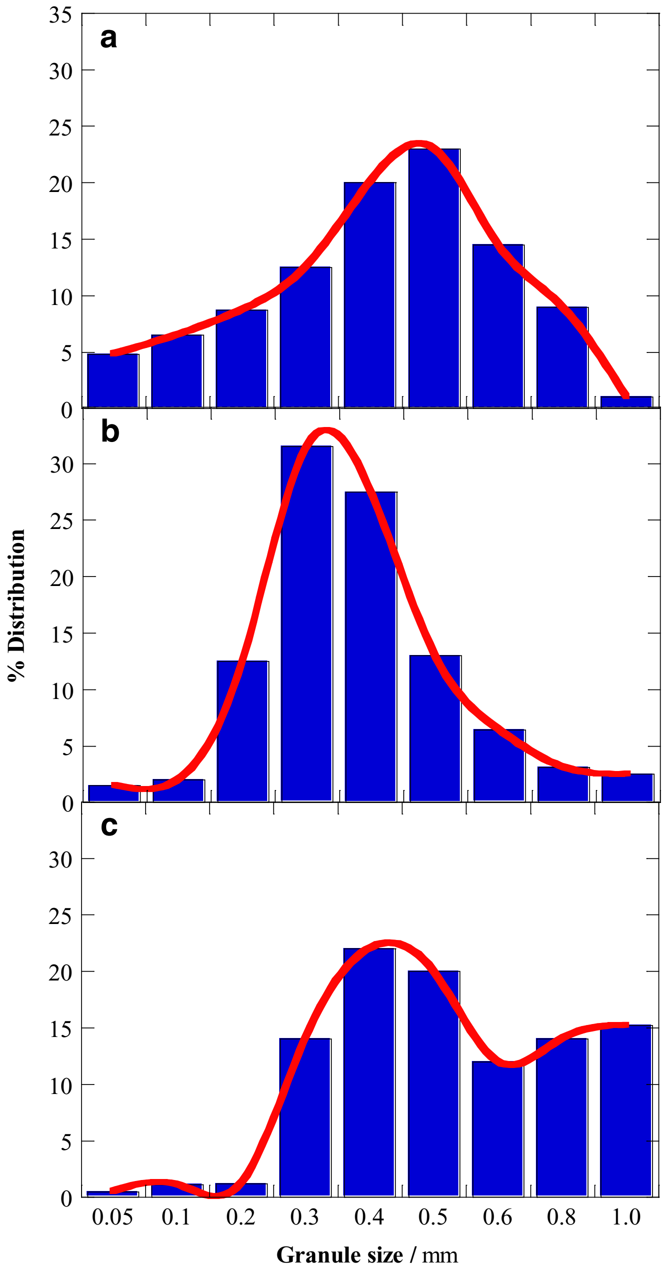

Fig. 6. Size distribution of granules obtained under experimental conditions of Fig. 5 at different $[Ca^{2+}]:[PO_4^{3-}]_T$ molar ratios: (a) 1.0:1.0, (b) 1.2:1.0, and (d) 1.4:1.0.

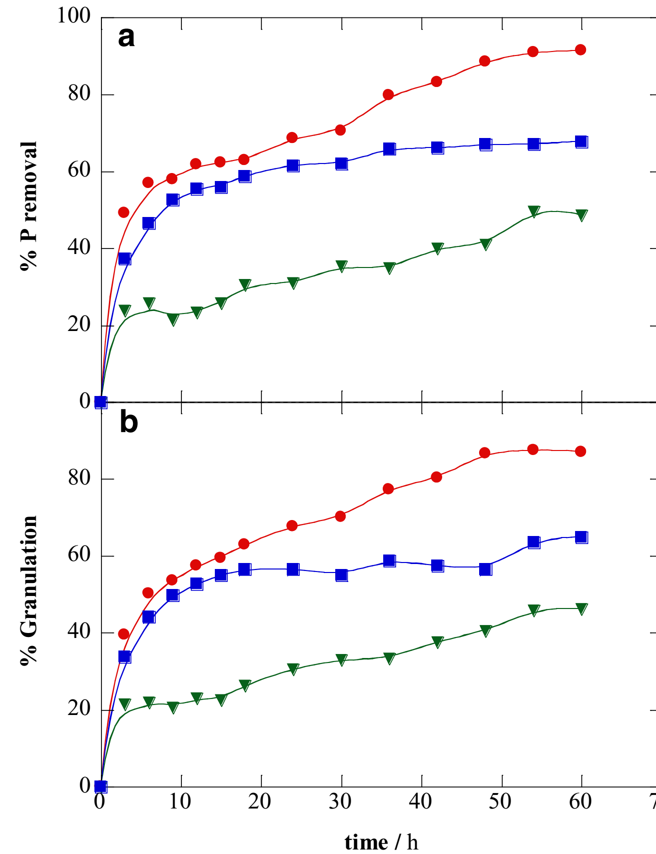

Fig. 7. Evolution of (a) phosphorus removal and (b) granulation percentages achieved by means of FBHC at pH 9.0 and molar ratio 1.2:1.0 $[Ca^{2+}]:[PO_4^{3-}]_T$ for different contents of phosphate: (▼) 500 mg/L, (■) 1000 mg/L and (●) 1500 mg/L.

precipitate insoluble calcium phosphate, operational pH should be encompassed in the range 5.0–14.0. Concentrations of hydrogen-phosphate and phosphate in solution define the minimum calcium requirements as precipitant to reach supersaturation conditions (Fig. 2b).

Fig. 3 depicts the percentage of granulation and the phosphorous removal of comparative experiences carried out at fixed molar ratio of 1.2:1.0 of $[Ca^{2+}]:[PO_4^{3-}]_T$ with an influent phosphate concentration of 1500 mg/L (15.8 mM) under an inflow rate of 20 mL/min (1.2 L/h) under different pH. The attained percentage of P-removal is always higher than the percentage of P-recovered independently of the pH conditions. This trend could be explained by the formation of fine nuclei that are not recoverable, diminishing the overall granulation efficiency.

Increasing percentages of 56.40%, 78.69% and 88.37% were obtained after 60 h of FBHC treatment at pH 6.0, 7.0 and 9.0, respectively. Increasing performance of FBHC process is associated to the speciation of phosphate. Alkaline influent pH incentivizes to reach supersaturation conditions due to the major presence of HPO_4^{2-} and PO_4^{3-}, which are the precursors of their respective insoluble calcium salts (reactions (4), (5)). Similar behavior on phosphate crystallization was previously reported regarding the obtaining of struvite [4,9,20] and magnesium phosphate [23]. Conversely, higher level of supersaturation under excessively alkaline conditions induces the preferential nucleation over crystal growth kinetics. At pH 11.0 the treated solution became more whitish and cloudy due to the formation of a colloidal suspension of fines precipitated, instead of the colorless solution obtained at pH 9.0. Formation of higher amounts of fines diminishes FBHC granulation recovery attaining only a poor 74.81%, although ~72% of the phosphorous could be removed by filtration after 5 min of treatment.

Size distribution of granules obtained at different pH provides valuable information on the applicability of FBHC to recovery calcium phosphates. Fig. 4 shows the granule size distribution, which under no circumstances were bigger than 2.0 mm. The crystals presented the characteristic spheroidal shape obtained in fluidized-bed reactors due to solid fluidization during crystal growth. Major crystals were obtained under more alkaline solutions where the major concentration of precipitates led to their agglomeration and crystal growth as deduced from the Gaussian distribution of sizes. Noteworthy is that under pH 11.0 highly heterogeneous distribution of crystal size was obtained.

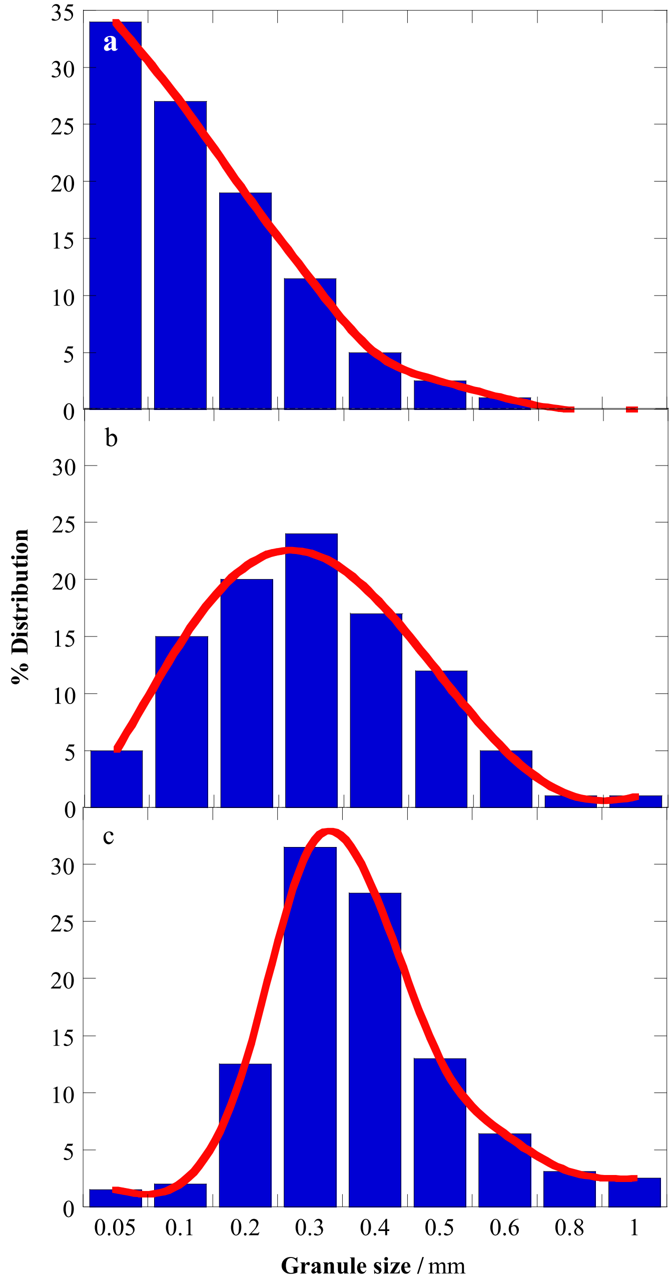

Fig. 8. Size distribution of granules obtained at different initial concentrations of phosphate: (a) 500 mg/L, (b) 1000 mg/L and (c) 1500 mg/L.

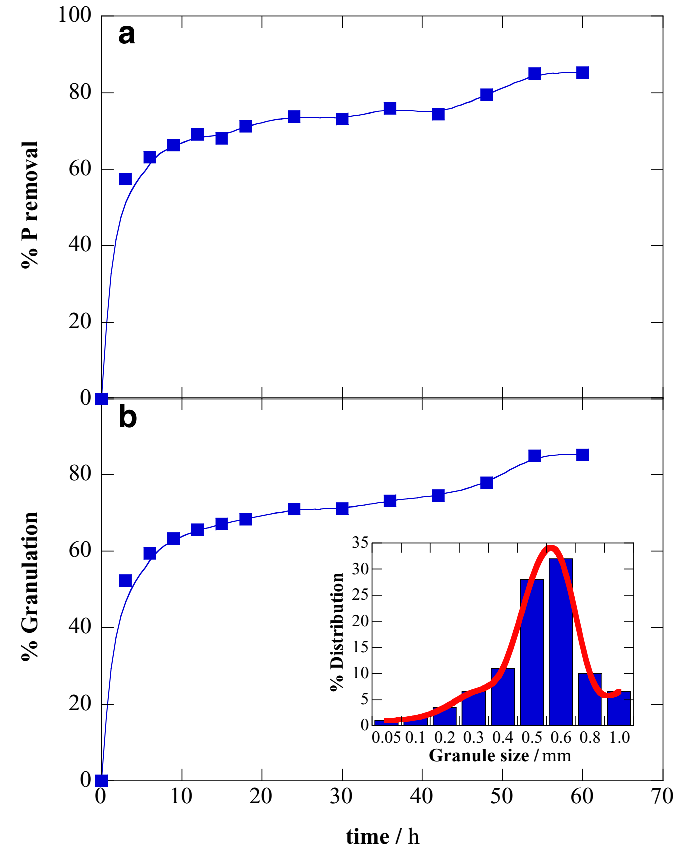

Fig. 9. Evolution of (a) phosphorus removal and (b) granulation percentages during the treatment of TFT/LCD effluent containing 7 mg/L of fluoride, 70 mg/L of nitrate, 550 mg/L of sulfate and 1500 mg/L of phosphate. Inset panel shows granule size distribution.

3.2. Effect of $[Ca^{2+}]$:$[PO_4^{3-}]_T$ molar ratio on the FBHC performance

The ratio between precipitant (Ca^{2+}) and pollutant (PO_4^{3-}) concentration could affect the performance of FBHC, as observed in FBC [4,30,31]. Phosphate recovery experiments were carried out under optimal pH 9.0, influent phosphate concentration of 1500 mg/L (15.8 mM), inflow rate of 20 mL/min at different $[Ca^{2+}]$:$[PO_4^{3-}]_T$ molar ratio.

Increase on $[Ca^{2+}]$ leads to a major phosphorous removal percentage at identical times of treatment (see Fig. 5) of 73.4%, 91.2% and 97.6% for ratios of 1.0:1.0, 1.2:1.0 and 1:4:1.0, respectively. This behavior is associated to the increase on the supersaturation due to the major concentration of precipitant $[Ca^{2+}]$. Similar trends were observed on the percentage of granulation, where higher crystallization percentages were attained for higher molar ratios of $[Ca^{2+}]$:$[PO_4^{3-}]_T$ in crescent order of 72.4% < 86.9% < 97.1% for 1.0:1.0, 1.2:1.0 and 1:4:1.0 $[Ca^{2+}]$:$[PO_4^{3-}]_T$ ratios, respectively. Further analysis of crystal size distribution (Fig. 6) demonstrated the favored crystal growth of brushite under greater ratios. As shown in Fig. 6b, a better Gaussian distribution was obtained at 1.2:1.0 $[Ca^{2+}]$:$[PO_4^{3-}]_T$ ratio than the wider range of crystals size distributions observed for 1.4:1.0 ratio. Even though the crystal recovery is slightly inferior, the obtaining of homogeneous size product is of higher interest for industrial purpose and commercialization. Therefore, the use of $[Ca^{2+}]$:$[PO_4^{3-}]_T$ ratio 1.2:1.0 was defined as optimum operational condition.

3.3. Recovery under different inlet concentrations of phosphate

Comparative experiments were conducted under optimal defined conditions of pH 9.0 and molar ratio 1.2:1.0 of $[Ca^{2+}]$:$[PO_4^{3-}]_T$ under 20 mL/min of influent containing phosphate concentration in the range found in industrial effluents of 500–1500 mg/L. From Fig. 7 can be concluded that low concentrations of 500 mg/L phosphate led to poor removals of 48.5% in comparison to 66.7% and 91.3% achieved at 1000 and 1500 mg/L of phosphate. The analysis of granules size distribution (Fig. 8) evidences higher crystal sizes for higher phosphate contents. Thereby, major concentrations lead not only to major precipitation and phosphorous removal from aqueous phase, but also enhance the crystal growth. However, it is important to remark that excessive concentrations could lead to preferential precipitation of large amounts of fine nuclei diminishing crystal growth.

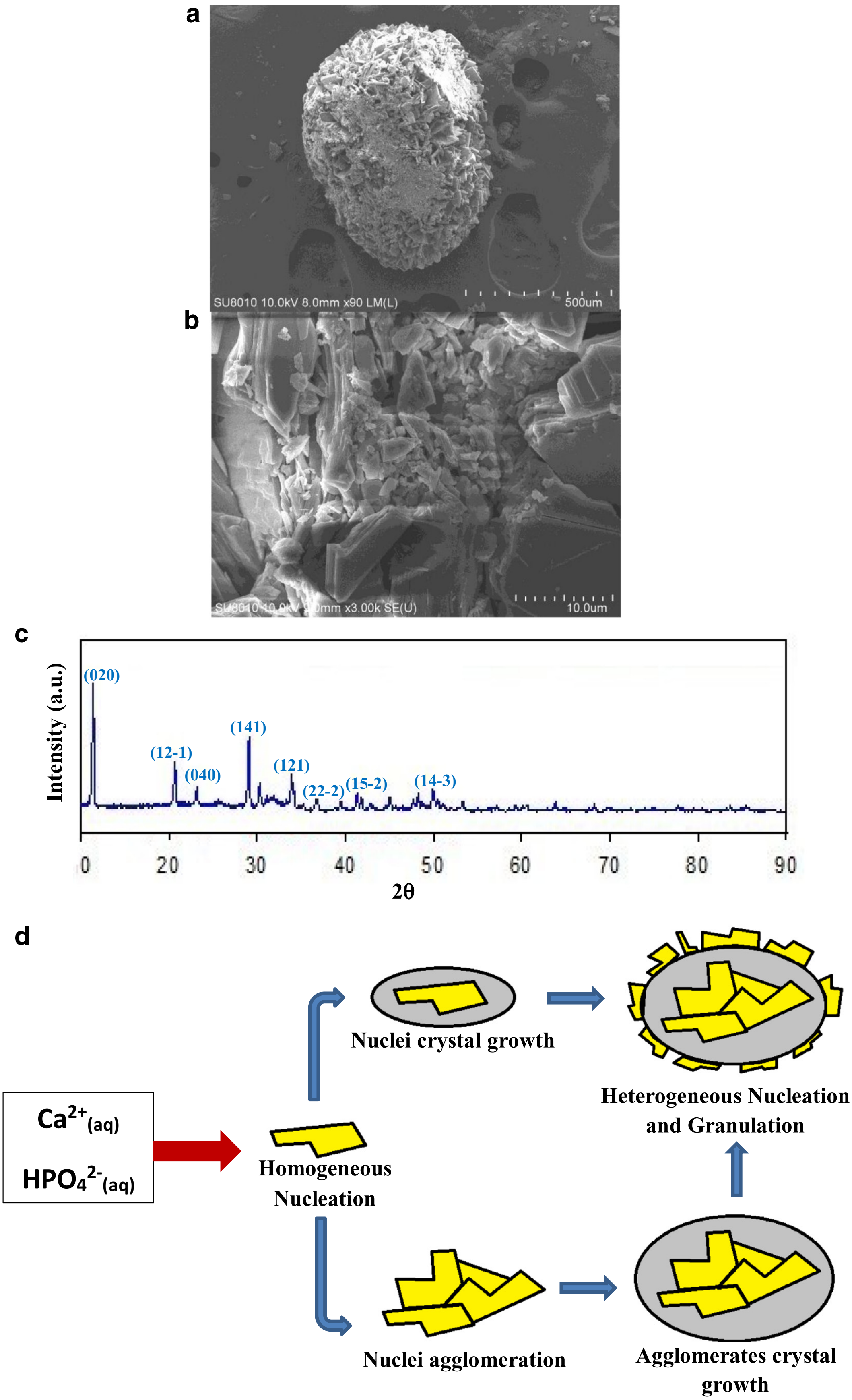

Fig. 10. (a,b) Scanning electron microscopy (SEM) image of the free-surface of spheroidal granules obtained. (c) X-ray diffractograms of granules. (d) Mechanisms involved on the formation of homogeneous crystals.

3.4. FBHC treatment of simulated TFT-LCD/photonics industry effluent

Taiwan is the largest worldwide supplier (∼ 40%) of transistor-liquid crystal display (TFT-LCD). Large volumes of water are consumed during TFT-LCD panels manufacturing [39,40]. High concentrations of phosphate (∼1500 mg/L) are present in these effluents due to the use of high amounts of phosphoric acid of electronic grade. Nevertheless, another anionic species are found in the industrial effluents due to the use of strong inorganic acids. TFT-LCD effluents present also appreciable concentrations of fluoride (∼7 mg/L), nitrate (∼70 mg/L) and sulfate (∼550 mg/L) [41]. These anionic species could compromise the overall performance and recovery of phosphate from industrial effluents. To evaluate the influence of complex water matrices treatment, a synthetic effluent of TFT-LCD industry considering the maximum concentrations of competitive anions (7 mg/L of F^-, 70 mg/L of NO_3^- and 550 mg/L of SO_4^{2-}) was treated by FBHC under optimal conditions of 1500 mg/L of PO_4^{3-}, pH 9.0 and molar ratio 1.2:1.0 of $[Ca^{2+}]$:$[PO_4^{3-}]_T$ at 20 mg/L influent. Fig. 9 shows that similar phosphorous removal is attained when the simulated effluent is treated, attaining 85.2% removal instead of 91.3% of the ideal solution (∼6.1% difference). Meanwhile, similar granulation is observed with values ∼85–86% in both cases. These results are highly encouraging since it could be inferred that the addition of competing species does not affect severely the FBHC performance, recovering brushite with average granule size of 0.5–0.6 mm (inset panel Fig. 9).

If we analyze the possible interference of typical anionic species in TFT-LCD effluents, different K_{sp} of insoluble products should be considered. Calcium nitrate is a highly soluble salt in water (1210 g/L at 20 °C) which could only modify the overall ionic strength of the solution. Calcium sulfate ($K_{sp} = 4.93 \times 10^{-5}$) is soluble in water (2.1 g/L at 20 °C) in the conditions of the industrial effluent and its influence can be neglected.

On the other hand, calcium fluoride is quite insoluble with a $K_{sp} = 3.90 \times 10^{-11}$ and an estimated solubility of 16 mg/L at 20 °C in water. Even though K_{sp} of phosphate salts are several orders of magnitude lower, the formation of CaF_2 is the only precipitation equilibria that could be considered as competing reaction under experimental conditions. However, CaF_2 crystals were not identified as individual granules or co-precipitated with brushite granules recovered. This trend can be explained by the higher concentration of phosphate (15 mM) in comparison to fluoride (0.37 mM), which favors thermodynamically and kinetically brushite precipitation in FBHC reactor. Therefore, the decrease of 6% on phosphate removal can be associated to the increase of ionic strength that affects the solubility of phosphate salts [42,43]. The high removals of phosphorus attained are comparable to the performance of other removal technologies [44,45]. But FBHC is more competitive non-solid waste technology due to the higher recovery of pure granules [44,45].

3.5. Crystals characterization

The crystals obtained by FBHC process under optimum conditions of treatment for influents of 1500 mg/L of phosphate at pH 9.0 with a ratio of 1.2:1.0 of $[Ca^{2+}]$:$[PO_4^{3-}]_T$ were further characterized. The SEM micrograph of Fig. 10a and b. show the typical morphological structure of petal-like particles of brushite that form parallelogram shapes stacked in multiple layers. While the granules are composed of clusters or aggregations of these petal-like crystals [24,25]. This result suggests the following mechanism (Fig. 10c): (i) formation of nuclei, (ii) aggregation of fine nucleis and (iii) crystal growth.

The X-ray diffractogram demonstrated that the granules are composed by calcium hydrogenphosphate dihydrated crystals ($CaHPO_4 \bullet 2H_2O$) showing the characteristic planes of brushite monoclinic crystal phase. Similar results were observed during the analysis of granules obtained during the treatment of synthetic TFT-LCD effluent. From these valuable data, it should be concluded that FBHC at pH 9.0 does not involve the formation of the most insoluble calcium phosphate expected from Fig. 2 according to reaction (5), but solely the nucleation and crystal growth of brushite according to reaction (4).

4. Conclusions

Applicability of FBHC to recover phosphate from aqueous bodies has been demonstrated. Operational parameters presented a marked influence on granulation performance. Optimal treatment conditions were defined as 1500 mg/L of phosphate inlet at pH 9.0 with a ratio of 1.2:1.0 of $[Ca^{2+}]$:$[PO_4^{3-}]_T$. Despite higher percentages of granulation were found using a higher ratio of precipitant and phosphate, the crystals obtained presented a wide distribution of heterogeneous sizes. Since FBHC process aimed not only phosphate removal but also its recovery for industrial manufacturing purposes, the formation of homogeneous crystals is of high relevance. The crystals characterization allowed identifying only brushite crystal phase composition, showing that pure calcium hydrogenphosphate crystals can be recovered efficiently by this novel technology. The treatment of synthetic effluents of TFT/LCD industry evidenced a small influence of water matrix. Therefore, FBHC emerges as a potential remediation water treatment technology to recover/revalorize phosphate residues from waste streams in comparison to existing technologies.

Acknowledgments

The authors would like to thank the Ministry of Science and Technology, Taiwan, for financially supporting this research under Contract No. 102-2221-E-041-001-MY3.

References

[1] Cordell D, Rosemarin A, Schröder JJ, Smit AL. Towards global phosphorus security: a systems framework for phosphorus recovery and reuse options. Chemosphere 2011;84:747–58.
[2] Cornel P, Schaum C. Phosphorus recovery from wastewater: needs, technologies and costs. Water Sci Technol 2009;59:1069–76.
[3] Tugaoen HO, Garcia-Segura S, Hristovski K, Westerhoff P. Challenges in photocatalytic reduction of nitrate as a water treatment technology. Sci Total Environ 2017;599-600:1524–51.
[4] de Luna MDG, Abarca RRM, Su C-C, Huang Y-H, M-C Lu. Multivariate optimization of phosphate removal and recovery from aqueous solution by struvite crystallization in a fluidized-bed reactor. Desalin Water Treat 2015;55:496–505.
[5] Liu Y, Kwag J-H, Kim J-H, Ra C. Recovery of nitrogen and phosphorus by struvite crystallization from swine wastewater. Desalination 2011;277:364–9.
[5] Battistoni P, Boccadoro R, Fatone F, Pavan P. Auto-nucleation and crystal growth of struvite in a demonstrative fluidized bed reactor (FBR). Environ Technol 2005;26:975–82.
[6] Metha CM, Batstone DJ. Nucleation and growth kinetics of struvite crystallization. Water Res 2013;47:2890–900.
[8] Seckler MM, Bruinsma OSL, van Rosmalen GM. Calcium phosphate precipitation in a fluidized bed in relation to process conditions: a black box approach. Water Res 1996;30:1677–85.
[9] Erickson AJ, Gulliver JS, Weiss PT. Capturing phosphates with iron enhanced sand filtration. Water Res 2012;46:3032–42.
[10] Kim HC. High-rate MIEX filtration for simultaneous removal of phosphorous and membrane foulants from secondary effluent. Water Res 2015;69:40–50.
[11] Tran N, Drogui P, Blais JF, Mercier G. Phosphorous removal from spiked municipal wastewater using either electrochemical coagulation or chemical coagulation as tertiary treatment. Sep Purif Technol 2012;95:16–25.
[12] Lacasa E, Cañizares P, Sáez C, Fernández FJ, Rodrigo MA. Electrochemical phosphates removal using iron and aluminium electrodes. Chem Eng J 2011;172:137–43.
[13] Garcia-Segura S, Eiband MMSG, Melo JV, Martínez-Huitle CA. Electrocoagulation and advanced electrocoagulation processes: a general review about the fundamentals, emerging applications and its association with other technologies. J Electroanal Chem 2017;801:267–99.
[14] Ottosen LM, Jensen PE, Kirkelund GM. Phosphorous recovery from sewage sludge ash suspended in water in a two-compartment electrodialytic cell. Waste Manag 2016;51:142–8.

[15] Porada S, Zhao R, van der Wal A, Presser V, Biesheuvel PM. Review on the science and technology of water desalination by capacitive deionization. Prog Mater Sci 2013;58:1388–1442.
[16] Delgadillo-Mirquez L, Lopes F, Taidi B, Pareau D. Nitrogen and phosphate removal from wastewater with a mixed microalgae and bacteria culture. Biotechnol Rep 2016;11:18–26.
[17] Wang X-X, Wu Y-H, Zhang T-Y, Xu X-Q, Dao G-H, H-Y Hu. Simultaneous nitrogen, phosphorous, and hardness removal from reverse osmosis concentrate by microalgae cultivation. Water Res 2016;94:215–24.
[18] Battistoni P, Pavanm P, Prisciandaro M, Cecchi F. Struvite crystallization: a feasible and reliable way to fix phosphorus in anaerobic supernatants. Water Res 2000;34:3033–41.
[19] Forrest AL, Fattah KP, Mavinic DS, Koch FA. Optimizing struvite production for phosphate recovery in WWTP. J Environ Eng 2008;134:395–402.
[20] Iqbal M, Bhuiyan H, Mavinic DS. Assessing struvite precipitation in a pilot-scale fluidized bed crystallizer. Environ Technol 2008;29:1157–67.
[21] Shih Y-J, Chang H-C, Huang Y-H. Reclamation of phosphorus from aqueous solutions as alkaline earth metal phosphate in a fluidized-bed homogeneous crystallization (FBHC) process. J Taiwan Inst Chem Eng 2016;62:177–86.
[22] Su C-C, Reano RL, Dalida MLP, M-C Lu. Barium recovery by crystallization in a fluidized-bed reactor: effects of pH, Ba/P molar ratio and seed. Chemosphere 2014;105:100–5.
[23] Su C-C, Dulfo LD, Dalida MLP, M-C Lu. Magnesium phosphate crystallization in a fluidized-bed reactor: effects of pH, Mg:P molar ratio and seed. Sep Purif Technol 2014;125:90–6.
[24] Tamimi F, Sheikh Z, Barralet J. Dicalcium phosphate cements: Brushite and monetite. Acta Biomater 2012;8:474–87.
[25] Oliveira C, Georgieva P, Rocha F, Ferreira A, de Azevedo SF. Dynamical model of brushite precipitation. J Cryst Growth 2007;305:201–10.
[26] Monma H, Kamiya T. Preparation of hydroxyapatite by the hydrolysis of brushite. J Mater Sci 1987;22:4247–50.
[27] Guillard D, Lewis AE. Nickel carbonate precipitation in a fluidized-bed reactor. Ind Eng Chem Res 2001;40:5564–9.
[28] Salcedo AFM, Ballesteros FC, Vilando AC, M-C Lu. Nickel recovery from synthetic Watts bath electroplating wastewater by homogeneous fluidized bed granulation process. Sep Purif Technol 2016;169:128–36.
[29] Chung J, Jeong E, Choi JW, Yun ST, Maeng SK, Hong SW. Factors affecting crystallization of copper sulfide in fed-batch fluidized bed reactor. Hydrometallurgy 2015;152:107–12.
[30] Chen C-S, Shih Y-J, Huang Y-H. Remediation of lead (Pb(II) wastewater through recovery of lead carbonate in a fluidized-bed homogeneous crystallization (FBHC) system. Chem Eng J 2015;279:120–8.
[31] de Luna MDG, Bellotindos LM, Asiao RN, Lu M-C. Removal and recovery of lead in a fluidized-bed reactor by crystallization process. Hydrometallurgy 2015;155:6–12.
[32] Aldaco R, Garea A, Irabien A. Fluoride recovery in a fluidized bed: crystallization of calcium fluoride on sílica sand. Ind Eng Chem Res 2006;45:796–802.
[33] Aldaco R, Garea A, Irabien A. Calcium fluoride recovery from fluoride wastewater in a fluidized bed reactor. Water Res 2007;41:810–18.
[34] Huang Y-H, Shih Y-J, Chang C-C, Chuang S-H. A comparative study of phosphate removal technologies using adsorption and fluidized bed crystallization process. Desalin Water Treat 2011;33:351–6.
[35] Su C-C, Abarca RRM, de Luna MDG, Lu M-C. Phosphate recovery from fluidized-bed wastewater by struvite crystallization technology. J Taiwan Inst Chem Eng 2014;45:2395–402.
[36] Garcia-Segura S, Bellotindos LM, Huang Y-H, Brillas E, M-C Lu. Fluidized-bed Fenton process as alternative wastewater treatment technology- A review. J Taiwan Inst Chem Eng 2016;67:211–25.
[37] Werther J. Fluidized-bed reactors in Ullman's encyclopedia of industrial chemistry. Wiley: USA; 2007.
[38] He Z, Honeycutt CW. A modified molybdenum bluemethod for orthophosphate determination suitable for investigating enzymatic hydrolysis of organic phosphates. Commun Soil Sci Plant Anal 2005;36:1373–83.
[39] Hung S-W. Competitive strategies for Taiwan's thin film transistor-liquid crystal display (TFT-LCS) industry. Technol Soc 2006;28:349–61.
[40] Colades JI, de Luna MDG, Su C-C, M-C Lu. Treatment of thin film transistor-liquid crystal display (TFT-LCD) wastewater by the electro-Fenton process. Sep Purif Technol 2015;145:104–12.
[41] Gunawan E, Warmadewanthi X, Liu JC. Removal of phosphate and fluoride from optoelectronic wastewater by calcite. Int J Environ Technol Manag 2010;12:308–21.
[42] Willey JD. The effect of ionic strength on the solubility of an electrolyte. J Chem Edu 2004;81:1644–6.
[43] Burgot J-L. Ionic equilibria in analytical Chemistry. Chapter 32: dependence of the solubility on the solution's ionic strength and on the presence of common ions: superimposition of several precipitation equilibria. USANew York: Springer-Verlag; 2012. p. 619–31.
[44] Cieslik B, Konieczka P. A review of phosphorus recovery methods at various steps of wastewater treatment and sewage sludge management. The concept of "no solid waste generation" and analytical methods. J Clean Prod 2017;142:1728–40.
[45] Kataki S, West H, Clarke M, Baruah DC. Phosphorus recovery as struvite: Recent concerns for use of seed, alternative Mg source, nitrogen conservation and fertilizer potential. Resour Conserv Recycl 2016;107:142–56.